Rays, Beams, and Modes Pertaining to the Excitation of Dielectric Waveguides

LEOPOLD B. FELSEN, FELLOW, IEEE, AND SANG-YUNG SHIN

Abstract—**The two-dimensional problem of excitation of an inhomogeneous dielectric layer by a Gaussian beam is considered, with emphasis on useful representations that treat the field either in terms of multiple reflections or in terms of guided modes. A recently developed method is employed whereby the beam fields are generated from line source fields by assigning a complex value to the source coordinates. When applied to the asymptotic solution for the line source field, this procedure furnishes a simple and quantitative relation between line-source-excited ray optics and paraxial beam optics. It also clarifies the role of lateral ray and beam shifts for reflection at a boundary with incidence-angle-dependent reflection coefficient, especially when multiply reflected fields are converted into modal form. Results are given for beams which are reflected at both boundaries, reflected at one boundary and refracted before reaching the other boundary, and trapped by refraction without reaching either boundary. In the first case, conversion to modal form is more convenient at large distances whereas in the latter case, paraxial beam tracking is preferable.**

I. INTRODUCTION

FOR a better understanding of relevant wave phenomena, there has been a concern in the literature on integrated and fiber optics with the relation between rays and modes in dielectric waveguides, with the ray-optical interpretation of modal phase and group velocity, with the propagation of beams, and with other aspects of modal propagation [1], [2]. The purpose of the present paper is to present a unified treatment of these phenomena by considering explicitly the problem of excitation of a dielectric waveguide by a localized source, such as a line or point source and a well-collimated Gaussian beam. It is found that consideration of the source problem interrelates various facets of wave propagation that have previously been considered separately and individually. These facets include the tracking of an obliquely incident beam by multiple reflection, the significance of lateral ray and beam shifts in the reflection process, the conversion of multiply reflected fields into waveguide modes and the role of the lateral shifts in the conversion process, the direct excitation of waveguide modes, and finally, the range where one field representation (multiply reflected or modal) is preferable over the other.

The specification of a localized source is essential to the present study, since the resulting excitation of a spectrum of wavenumbers makes possible the systematic exploration of the wave processes alluded to above. For two-dimensional or three-dimensional wave problems, a line source or point source, respectively, forms a suitable prototype. Such sources, being omnidirectional, actually give rise to a richer variety of wave phenomena than those encountered when the wavenumber spectrum is narrowly confined, as in a well-collimated beam. However, by a recently developed method [3], [4], it is possible to convert incident cylindrical or spherical wave fields into two-dimensional or three-dimensional paraxial Gaussian beams, respectively, on replacing the real source coordinate by a complex value. Thus previously developed Green's functions for dielectric waveguides can be utilized directly for construction of field solutions when the incident excitation is a Gaussian beam. In following this procedure here, heavy reliance is placed on an earlier publication [5] dealing with rays, modes, ray-modal conversion, etc., of two-dimensional fields in an inhomogeneous layer with impedance walls, excited by an omnidirectional source or by a source with known far zone radiation pattern $f(\theta)$. For simplicity, the analysis will be restricted to the two-dimensional case, with only a brief mention of the generalization to three dimensions.

Turning now to the actual contents of this paper, we begin in Section II with a summary of the complex-source-point method when applied to a point or line source in free space; this demonstrates the ability to generate an incident Gaussian beam from a spherical or cylindrical wave by assigning to the source a complex location. To understand the effects of waveguide boundaries when a beam is injected through an open end (or through an opening in one of the walls), we consider first a homogeneously filled, perfectly conducting, multimode parallel plane waveguide (Section III). By using Green's function representations either in the form of a mode series or an image series, and then employing the complex-source-point method, one obtains at once the modal excitation coefficients due to an incident beam, the fields described by tracking of multiple reflections, and an assessment of parameter ranges where one representation is preferable to the other. It will come as no surprise that the most strongly excited waveguide modes are those whose plane

Manuscript received May 17, 1974; revised July 25, 1974. This work was supported in part by the National Science Foundation under Grant GK10917, and in part by the Joint Services Electronics Program under Contract F44620-69-C-0047. It forms part of a dissertation to be submitted by S. Y. Shin in partial fulfillment of the requirements for the Ph.D. degree. The manuscript was prepared while one of the authors (L. B. Felsen) was with the Institute for Electromagnetic Wave Research, National Research Council, Florence, Italy.

The authors are with the Department of Electrical Engineering and Electrophysics, Polytechnic Institute of New York, Farmingdale, N. Y. 11735.

wave constituents propagate in directions θ_m closest to that of the incident beam. It is also found that with respect to modal excitation, the beam acts like a directive source with a radiation pattern that decays exponentially away from the beam axis.

In Section IV the problem is generalized to an inhomogeneous layer bounded by surface impedance walls. As mentioned earlier, this model is chosen because all of the relevant formulas pertaining to excitation by an isotropic or directional line source have already been developed [5]. These formulas, summarized in Section IV-A, comprise rays and modes which 1) are trapped in the vicinity of the layer axis by refraction due to the medium inhomogeneity, 2) are reflected at one boundary but refracted before reaching the other boundary, and 3) are reflected at both boundaries. Cases 2) and 3) involve lateral shifts of reflected rays, which are discussed in detail. It is found that while lateral shifts should always be included in the description of reflection of rays emanating from a localized source, the effect of such shifts is generally insignificant when only a few reflections are involved; however, the correct description of the cumulative effect of many reflections, and especially, the conversion of multiply reflected ray fields into modal fields requires retention of lateral shifts. Since conventional geometric-optical tracking procedures for phase and amplitude of the quasi-optic field can easily be adapted to the laterally shifted paths [6], [7], this poses no hardship. The effect of replacing the real source point in the formulas of Section IV-A by a complex value is examined in Section IV-B. It is found that when the medium inhomogeneity can be neglected in the vicinity of the waist of the incident beam, the complex-source-point field decays in Gaussian fashion away from a central ray, the beam axis. Depending on the choice of the complex source point, the beam axis may belong to any of the categories 1), 2), and 3) noted above. The beam characteristics for these cases are discussed, together with the excitation of modal fields. In particular, it is shown that the paraxial beam field can be described completely in terms of parameters pertaining to the line-source-excited field on a ray coincident with the beam axis. This observation provides a direct and quantitative correspondence between paraxial beam optics and line-source-excited ray optics.

The results obtained for beam excitation of an inhomogeneous layer with impedance walls apply also when the layer boundaries are formed by a discontinuity in refractive index, provided that the beam is incident at an angle that assures the occurrence of total reflection at the boundaries (or continuous refraction before reaching the boundaries). In that event, excitation of the continuous mode spectrum is negligible (see Appendix III). Treatment of the discrete mode spectrum is the same as for the layer with impenetrable impedance walls provided only that the impedance-wall reflection coefficients are replaced by the interface reflection coefficients. These considerations are summarized in Section IV-C. General conclusions to be drawn from this study are presented in Section V.

II. THE INCIDENT BEAM FIELD

The time-harmonic scalar three-dimensional Green's function, which satisfies the radiation condition in a homogeneous unbounded lossless medium with wavenumber k, is given by

$$G_f(\mathbf{r},\mathbf{r}') = \frac{\exp(ikQ)}{4\pi Q} \tag{1}$$

where Q is the distance from the source point $\mathbf{r}'$ to the observation point $\mathbf{r}$,

$$Q = |\mathbf{r} - \mathbf{r}'| = [(x-x')^2 + (y-y')^2 + (z-z')^2]^{1/2} \tag{1a}$$

and the time dependence $\exp(-i\omega t)$ has been suppressed. When the source point $\mathbf{r}'$ is assigned the complex value $\mathbf{r}_b' = (0,0,i\hat{b})$, $\hat{b} > 0$, the real distance Q is replaced by the complex distance

$$Q_b = [x^2 + y^2 + (z - i\hat{b})^2]^{1/2}, \qquad \operatorname{Re} Q_b > 0 \tag{2}$$

which may be approximated in the paraxial region near the z axis as

$$Q_b \sim z - i\hat{b} + \frac{x^2+y^2}{2(z-i\hat{b})} \qquad x^2 + y^2 \ll z^2 + \hat{b}^2 \tag{3}$$

and in the far zone as

$$Q_b \sim r - i\hat{b}\cos\theta \qquad r \gg k\hat{b}^2 \qquad r = (x^2+y^2+z^2)^{1/2} \tag{4}$$

where $\cos\theta = z/r$. Substitution of (3) or (4) into (1) shows that the complex-source-point solution $G_f(\mathbf{r},\mathbf{r}_b')$ represents in the region $z > 0$ a field that behaves like a rotationally symmetric Gaussian beam in the paraxial region about the beam axis z, with amplitude $\exp(k\hat{b})$ on the axis. The exponential dependence $\exp[-k(x^2+y^2)/2\hat{b}]$ in the $z = 0$ plane identifies that plane as the focal plane and $(2\hat{b}/k)^{1/2}$ as the commonly defined half width w_o at the waist of the beam. Retention of (2) in (1) provides an exact solution of the scalar wave equation that is valid at arbitrary observation points (except $z = 0$, $x^2 + y^2 = \hat{b}^2$) and satisfies via the assumption $\operatorname{Re} Q_b > 0$ the radiation condition at all observation angles at infinity (i.e., the fields are outgoing in $z < 0$ and $z > 0$); by alternative definitions of the principal branch of Q_b, one may generate a field that is incoming in $z < 0$ and outgoing in $z > 0$ and thereby describes a Gaussian beam for all z. Since we shall be interested only in the perturbation of the beam after it has passed through its focus, the specification $\operatorname{Re} Q_b > 0$ is adequate and describes in a simple manner the analytic continuation of Q from real $\mathbf{r}'$ to complex $\mathbf{r}_b'$; the field may accordingly be viewed as having been established by an equivalent source distribution that occupies the region $x^2 + y^2 \leq \hat{b}^2$ in the $z = 0$ plane.

It is easily verified that when the complex source point is chosen as

$$\mathbf{r}_b' = \mathbf{r}_o + i\hat{\mathbf{b}} \tag{5}$$

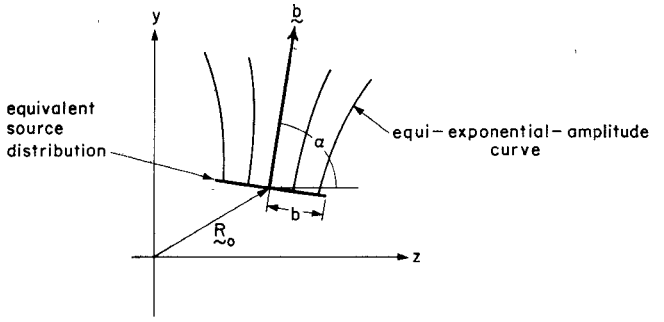

Fig. 1. Two-dimensional beam corresponding to $\tilde{G}_f(\boldsymbol{R}, \boldsymbol{R}_o + i\boldsymbol{b})$. The focus lies at $\boldsymbol{R}_o$ and the beam axis along $\boldsymbol{b}$.

where $\boldsymbol{r}_o$ and $\hat{\boldsymbol{b}}$ are real vectors, the resulting field $G_f(\boldsymbol{r},\boldsymbol{r}_b')$ represents a beam whose focus is at $\boldsymbol{r}_o$ and whose axis is along $\hat{\boldsymbol{b}}$.

By analogous considerations (Fig. 1), one establishes for the two-dimensional (x-independent) case that the two-dimensional scalar Green's function

$$\tilde{G}_f(\boldsymbol{R},\boldsymbol{R}') = \tfrac{1}{4}iH_o^{(1)}(k\tilde{Q}) \qquad \tilde{Q} = [(y - y')^2 + (z - z')^2]^{1/2}, \tag{6}$$

furnishes a two-dimensional beam solution when the distance $\tilde{Q}$ from the real source point $\boldsymbol{R}' = (y',z')$ is replaced by the distance $\tilde{Q}_b$ from the complex source point $\boldsymbol{R}_b' = \boldsymbol{R}_o + i\boldsymbol{b}$. To achieve a collimated beam, it is assumed that $kb \gg 1$, where $b = |\boldsymbol{b}|$, so that the asymptotic approximation

$$\tilde{G}_f(\boldsymbol{R},\boldsymbol{R}_b') \sim \frac{\exp(ik\tilde{Q}_b + i\pi/4)}{2(2\pi k\tilde{Q}_b)^{1/2}}, \qquad \operatorname{Re}\tilde{Q}_b > 0 \tag{7}$$

is adequate. However, as for the three-dimensional case, $\tilde{G}_f(\boldsymbol{R},\boldsymbol{R}_b')$ in (6) is an exact solution of the two-dimensional wave equation.

Vector beam fields may be generated from expressions for the vector fields due to an electric or magnetic current element on replacing the real source point location $\boldsymbol{r}'$ by the complex value $\boldsymbol{r}_b'$ in (5). If the vector beam is to have a TEM field on the beam axis $\hat{\boldsymbol{b}}$, the orientation of the current element must be perpendicular to $\hat{\boldsymbol{b}}$ [4].

III. BEAM-TO-MODE CONVERSION IN A WAVEGUIDE WITH PERFECTLY CONDUCTING BOUNDARIES

To illustrate the mechanism of waveguide mode excitation when a beam is launched into a region with parallel plane boundaries, it is appropriate to consider first a homogeneously filled waveguide with perfectly conducting walls. For simplicity, we deal only with the two-dimensional case. Since the complex displacement of the source coordinate of an incident cylindrical wave generates an incident beam that is Gaussian in the paraxial region, the beam excitation of a parallel plane waveguide with boundaries at $y = 0, d$ follows at once from the known solution of the two-dimensional Green's function for that region by analytic continuation from $\boldsymbol{R}'$ to complex $\boldsymbol{R}_b'$. Two alternative representations are of interest. The first,

$$\tilde{G}_1(\boldsymbol{R},\boldsymbol{R}') = \frac{i}{d}\sum_{m=1}^{\infty} \sin\frac{m\pi y}{d}\sin\frac{m\pi y'}{d}\frac{\exp[ik\tau_m(z - z')]}{k\tau_m}, \qquad z > z' \tag{8}$$

where d is the waveguide height and

$$\tau_m = [1 - (m\pi/kd)^2]^{1/2}, \qquad \operatorname{Im}\tau_m \geq 0,$$

expresses the field as a superposition of guided modes. The second,

$$\begin{aligned}\tilde{G}_1(\boldsymbol{R},\boldsymbol{R}') = \frac{i}{4}\sum_{s=0}^{\infty} \{&H_o^{(1)}(kR_{s1}) + H_o^{(1)}(kR_{s2}) \\ &- H_o^{(1)}(kR_{s3}) - H_o^{(1)}(kR_{s4})\}\end{aligned}$$

$$\begin{aligned}R_{s1} &= \{(z - z')^2 + (2sd + y - y')^2\}^{1/2}\\ R_{s2} &= \{(z - z')^2 + (2(s + 1)d + y' - y)^2\}^{1/2}\\ R_{s3} &= \{(z - z')^2 + (2sd + y + y')^2\}^{1/2}\\ R_{s4} &= \{(z - z')^2 + (2(s + 1)\,d - y - y')^2\}^{1/2}\end{aligned} \tag{9}$$

expresses the field as a superposition of image fields in an unbounded medium. The Green's function $\tilde{G}_1$ vanishes on the waveguide boundaries and is therefore proportional to the single-component electric field E_x.

To convert the incident cylindrical wave into a Gaussian beam with focus at (y_o,z_o) and axis inclined at an angle α with respect to z, we let

$$y' \to y_b' = y_o + ib\sin\alpha \qquad z' \to z_b' = z_o + ib\cos\alpha, \qquad b > 0, \qquad 0 < \alpha < \tfrac{1}{2}\pi \tag{10}$$

to obtain from (8), for $z > z_o$,

$$\begin{aligned}\tilde{G}_1(\boldsymbol{R},\boldsymbol{R}_b') = \frac{1}{2d}\sum_{m=1}^{\infty} \sin\frac{m\pi y}{d}\frac{\exp[ik\tau_m(z - z_o)]}{k\tau_m}\\ \cdot[\exp(im\pi y_o/d)\exp(kb\cos(\theta_m + \alpha))\\ - \exp(-im\pi y_o/d)\exp(kb\cos(\theta_m - \alpha))]\end{aligned} \tag{11}$$

where $\theta_m = \cos^{-1}\tau_m = \sin^{-1}(m\pi/kd)$ is the propagation angle, measured counter-clockwise from the positive z axis, of the constituent plane waves that synthesize the mth mode. The series is convergent provided that the exponential terms decay as $m \to \infty$. Since $\tau_m \to i(m\pi/kd)$ as $m \to \infty$, this implies the restriction

$$z > z_o + b\sin\alpha \tag{12}$$

on the analytically continued Green's function in (11); i.e., the axial coordinate of the observation point must be large enough to be outside the equivalent source distribution for the beam (see Fig. 1). Evidently, the mth propagating mode is optimally excited when the beam direction α coincides with the mode angle θ_m. For a highly collimated beam with large kb and for $\alpha \not\approx 0$, one may omit the first term inside the square brackets in (11) to obtain

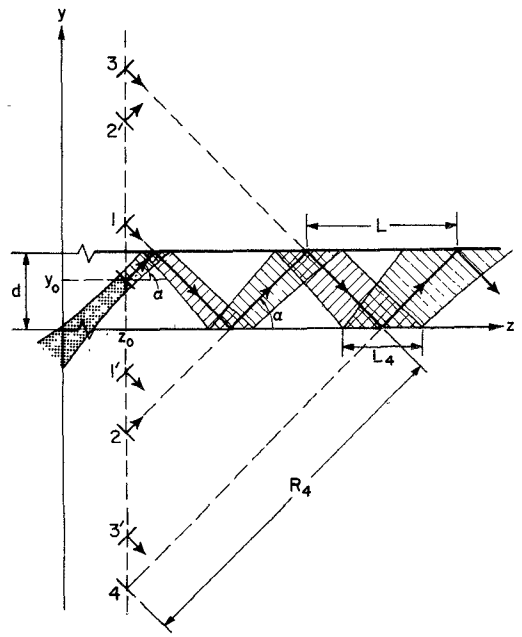

Fig. 2. Beam excitation of parallel plane waveguide with perfectly conducting walls. In the image representation, the primed images may be ignored. After N reflections the beam width is $L_N = 2(2/kb)^{1/2}R_N/\sin\alpha$. The multiply reflected beam is shown shaded. When the beam is injected from the outside (see dotted portion of the incident beam), the results in (9), with (10), remain applicable provided that the illumination at the edges is negligible.

$$\bar{G}_1(\boldsymbol{R},\boldsymbol{R}_b') \sim \sum_{m=1}^{\infty} \sin(ky\sin\theta_m)\exp(ikz\cos\theta_m)A_m \tag{13}$$

$$A_m = \exp[-ik(y_o\sin\theta_m + z_o\cos\theta_m) + kb\cos(\theta_m - \alpha)] \cdot \frac{(-1)}{2kd\cos\theta_m} \tag{13a}$$

where A_m is the mth mode excitation coefficient.

When (10) is employed in the image representation (9), the field in the waveguide region is synthesized by superposition of image beam contributions which account for the effects of multiple reflections (Fig. 2). Since the beam source is highly directive, the field is confined to the vicinity of the multiply reflected beam axis. By this consideration, one may omit the primed images altogether; their contribution in the region $0 \leq y \leq d$ is negligible when $\alpha \not\approx 0$ (this corresponds to the transition from (11) to (13)). Even the unprimed images contribute selectively and may be ignored when the observation point lies far from those portions of the multiply reflected beam axis corresponding to them. If it is adequate to disregard fields whose exponential amplitude lies below a prescribed level, the fields of interest are confined to the shaded region in Fig. 2. One notes that a single term from the series (9), with (10), is adequate to describe the field in any of the singly shaded portions, while two terms are adequate in overlapping shaded regions; the field in the unshaded portions is so small that it can be neglected. If the waveguide is wide enough to permit the propagation of many modes, the image representation (9) is preferable over the modal representation (11) or (13) as long as there is little or no overlap among the multiply reflected beams. Since the $(1/e)$ angular beam width in the far zone of any of the image sources is $\theta_w = 2(2/kb)^{1/2}$, the projected width L_N, parallel to the z-axis, of the beam originating at the Nth image (i.e., after N reflections) is

$$L_N = 2(2/kb)^{1/2}R_N/\sin\alpha \tag{14}$$

where R_N is the distance along the axis of the Nth image beam from its focus to the waveguide region (see Fig. 2). When L_N exceeds the interval $L = 2d\cot\alpha$ between successive reflections of the beam axis (see Fig. 2), the multiply reflected beam can no longer be resolved. As the observer moves down the guide to $z > z_N$, where the vicinity of z_N is defined by $L \approx L_N$, the field is synthesized by an ever increasing number of image contributions in (9). The collective effect of these image fields is eventually represented more compactly by the modal sum in (13). The modal sum thus accounts for the accumulation of many multiple reflections of rays whose initial direction lies within an angular interval of $O(\theta_w)$ about the beam axis $\theta = \alpha$. The direct conversion of the image sum into the modal sum may be accomplished by the Poisson transformation, which thus provides the means of passing from one representation to the other. Since the image representation (9) is intimately related to a ray-optical treatment (use of the asymptotic form for the Hankel functions (see (7)) actually reduces (9) to the ray-optical solution constructed by tracking multiply reflected rays), the Poisson transformation permits the conversion of ray solutions into modal solutions and, via the analytic continuation specified in (10), the conversion of beam solutions into modal solutions. This aspect is exploited in the next section.

Although in the preceding discussion the beam source is located in the interior of an infinite waveguide, one may use the same results when the waveguide is open-ended and the beam is injected from the outside, with the focus lying inside the parallel plane region (see Fig. 2). The validity of this statement follows from the highly directive properties of the incident beam. If the focus lies outside the parallel plane region, a divergent incident beam may be regarded as being generated by one of the image sources. When necessary, the interaction of an incident beam with the edges of an open-ended waveguide can be accounted for by use of complex source coordinates in a ray-optical treatment of the edge diffraction problem, but this will not be considered here [4].

It is appropriate to mention also a direct procedure for constructing the fields excited in a waveguide by an incident beam. From (7), (10), and the two-dimensional equivalent of (4) (see also Fig. 1), it is noted that the beam may be regarded as a distributed source with far zone radiation pattern

$$f(\theta) = \exp[kb\cos(\alpha - \theta)] \tag{15}$$

where $\theta = \alpha$ defines the beam axis. It is known that when a source distribution with far zone pattern $f(\theta)$ is placed

at the location $\boldsymbol{R}_o$ into a parallel plane waveguide, the field in the waveguide is given by [5]

$$\bar{G}_1(\boldsymbol{R},\boldsymbol{R}_o) = \frac{1}{2d}\sum_{m=1}^{\infty} \sin\frac{m\pi y}{d}\,\frac{\exp\left[ik\tau_m(z-z_o)\right]}{k\tau_m} \cdot\left[\exp\left(im\pi y_o/d\right)f(-\theta_m) - \exp\left(-im\pi y_o/d\right)f(\theta_m)\right] \tag{16}$$

where θ_m is the previously defined modal propagation angle and z is restricted to values outside the source region. Since the latter requirement is the same as (12), it is evident that (15) and (16) yield the solution (11) that was obtained by the complex-source-point procedure. Thus the modal excitation problem may also be approached by viewing the beam as a highly directive source, but this procedure lacks the versatility of the complex-source-point method for studying other aspects of the beam problem.

If $\bar{G}_2$ denotes the Green's function whose normal derivative vanishes on the boundary (i.e., $\bar{G}_2$ is proportional to a single-component magnetic field H_x), the expression in (8) is modified by the change of sines to cosines and extension of the summation from $m = 0$ to $m = \infty$; an additional factor (1/2) accompanies the $m = 0$ term. In the image representation (9), the minus signs are changed to plus. Correspondingly, the complex-source-point solution (11) contains an $m = 0$ term, has the sine replaced by cosine, and the minus sign between the two terms inside the square brackets replaced by plus (the modifications apply also to (16)). When $\alpha \not\approx 0$, this leads instead of (13) to

$$\bar{G}_2(\boldsymbol{R},\boldsymbol{R}_b') \sim \tfrac{1}{2}\bar{A}_o \exp\left(ikz\right) + \sum_{m=1}^{\infty} \cos(ky\sin\theta_m) \cdot\exp\left(ikz\cos\theta_m\right)\bar{A}_m \tag{17}$$

where $\bar{A}_m = -A_m$. The image representation follows from the modified form of (9). The interpretation of these results is the same as for the polarization associated with $\bar{G}_1$ except that the present case admits of an axially propagating (TEM) mode with $\theta_m = 0$.

IV. BEAM-TO-MODE CONVERSION IN A BOUNDED INHOMOGENEOUS LAYER

The simple example in Section III of a homogeneously filled parallel plane waveguide with perfectly conducting walls has served to illustrate relevant propagation mechanisms when the incident field is a well-collimated Gaussian beam. These mechanisms remain operative in the more general case of a layer whose refractive index varies continuously in the transverse direction. Nonradiating guided modes in such a layer can exist due to trapping by an appropriate refractive index inhomogeneity and (or) due to the presence of discontinuous changes in refractive index; in weakly inhomogeneous media, the latter may be described by an incidence-angle-dependent plane wave reflection coefficient. As before, the analysis is performed by introducing a complex source point location into the expressions for the fields due to a line current. Since we are interested only in the excitation of nonradiating guided modes (for a discussion including the continuous spectrum, see Appendix III), it suffices to consider the problem of an inhomogeneously filled waveguide bounded by impedance walls. The mechanism of excitation of guided modes in such a structure by a highly directive beam remains applicable when the impenetrable surface impedance walls are replaced by penetrable boundaries across which the refractive index is discontinuous, provided that the incident beam at these boundaries is totally reflected and that the surface impedance reflection coefficient is replaced by the interface reflection coefficient. Since the impedance wall problem has been treated previously [5], relevant formulas can be extracted directly for the present discussion.

A. Line Source Field in an Inhomogeneous Layer with Impedance Walls

Line source excitation of an inhomogeneous layer with refractive index $n(y)$, bounded by impedance walls at $y = y_1$ and $y = y_2$, was previously formulated in terms of a continuous spectrum of plane waves with z dependence $\exp(ik\tau z)$, $-\infty < \tau < \infty$ [5, eq. (I.8)].[1] The resulting integral representation was then converted (by contour deformation about the pole singularities (zeros of the resonance denominator) in the integrand) into a series of modes guided along z [5, eq. (I.13)]; for the special case of $n = 1$ and perfectly conducting walls, this series reduces to the one in (8) (or its counterpart for $\bar{G}_2$). Alternatively, by series expansion of the resonance denominator, the plane wave spectral integral was represented as a series of simpler integrals [5, eqs. (I.20) and (I.21)], each of which describes a single reflected constituent in a multiple reflection decomposition of the line source field; for the special case in Section III, these integrals are recognized as Hankel functions and lead to the image representation in (9) (or its counterpart for $\bar{G}_2$). Assuming that $n(y)$ changes slowly over an interval equal to the local wavelength, the multiple reflection integral solutions were simplified by asymptotic approximations that provide a direct ray-optical interpretation.

For the mode series, the result for $z > z'$ was shown to be [5, eq. (I.13a)]

$$\bar{G}(\boldsymbol{R},\boldsymbol{R}') = \sum_m \frac{1}{-2ik\tau_m N_m^2}\,\Phi_m(y)\,\Phi_m(y')\exp\left[ik\tau_m(z-z')\right] \tag{18}$$

$$N_m^2 = \int_{y_1}^{y_2} \Phi_m^2(y)\,dy. \tag{18a}$$

The eigenfunctions $\Phi_m(y)$ satisfy the modal equation

$$\left\{\frac{d^2}{dy^2} + k^2\left[n^2(y) - \tau_m^2\right]\right\}\Phi_m(y) = 0 \tag{19}$$

[1] Equations in [5] are denoted by a prefix (I). The x coordinate in [5] has here been replaced by y.

subject to the boundary conditions

$$\frac{d\Phi_m}{dy} = \pm ikZ_{1,2}\Phi_m \qquad \text{at } y = y_{1,2} \tag{19a}$$

where $Z_{1,2}$ are constant surface impedances at $y = y_{1,2}$.

The multiple-reflection representation

$$\bar{G}(\boldsymbol{R},\boldsymbol{R}') = \sum_{j=1}^{4}\sum_{s=0}^{\infty} I_{sj}(\boldsymbol{R},\boldsymbol{R}') \tag{20}$$

involves integrals of the type (see [5, eq. (I.23)])

$$I_{sj}(\boldsymbol{R},\boldsymbol{R}') \sim \frac{i}{4\pi}\int \frac{\exp\left[ik\psi_{sj}(\boldsymbol{R},\boldsymbol{R}';\tau)\right]\exp\left\{iP_{sj}[\phi_1(\tau),\phi_2(\tau)]\right\}}{[n^2(y) - \tau^2]^{1/4}[n^2(y') - \tau^2]^{1/4}}\,d\tau \tag{20a}$$

wherein appropriate asymptotic forms of the wave functions have already been utilized and $\exp(i\phi_1)$ and $\exp(i\phi_2)$ are the plane wave reflection coefficients for the impedance boundaries at y_1 and y_2, respectively. Henceforth, the wall impedance is assumed to be nondissipative so that $\phi_{1,2}$ are real. The evaluation of (20a) by the stationary phase method can be performed in two ways, which differ by the inclusion, or not, of the second exponential in the phase of the integrand (note that the second exponential does not contain the large wavenumber k). When the second exponential is included in the phase, the result is as follows:

$$I_{sj} \sim S_{sj}(\tau_{sj})\exp\left[ik\psi_{sj}(\tau_{sj})\right]\exp\left\{iP_{sj}[\phi_1(\tau_{sj}),\phi_2(\tau_{sj})]\right\} \tag{21}$$

where the dependence on $\boldsymbol{R}$ and $\boldsymbol{R}'$ has been omitted. For $j = 1$, one has explicitly

$$\psi_{s1}(\tau_s) = \int_{y<}^{y>} [n^2(\xi) - \tau_s^2]^{1/2}\,d\xi + 2s\int_{y_1}^{y_2} [n^2(\xi) - \tau_s^2]^{1/2}\,d\xi + \tau_s(z - z') \tag{21a}$$

$$P_{s1}[\phi_1(\tau_{s1}),\phi_2(\tau_{s1})] = s[\phi_1(\tau_{s1}) + \phi_2(\tau_{s1})] \tag{21b}$$

$$S_{s1}(\tau_s) = \frac{\exp(i\pi/4)}{(8\pi k)^{1/2}}\left\{-[n^2(y) - \tau_s^2]^{1/2}[n^2(y') - \tau_s^2]^{1/2} \cdot\left[\frac{\partial^2\psi_{s1}}{\partial\tau^2} + \frac{s}{k}\frac{\partial^2}{\partial\tau^2}(\phi_1 + \phi_2)\right]_{\tau_s}\right\}^{-1/2} \tag{21c}$$

where $\partial^2\psi_{s1}/\partial\tau^2$ is calculated by direct differentiation of (21a). The value of τ_{si}, abbreviated as τ_s, is determined so as to assure that the ray originating at $\boldsymbol{R}'$ passes through the observation point $\boldsymbol{R}$. This requirement is met if τ_s satisfies the ray equation, which is identical with the condition for stationary points in the integrand of (20a):

$$\frac{\partial}{\partial\tau_s}\psi_{s1}(\tau_s) + \frac{s}{k}\left(\frac{\partial\phi_1}{\partial\tau_s} + \frac{\partial\phi_2}{\partial\tau_s}\right) = 0. \tag{22}$$

The classification of the ray paths depends on the relative orientation of source and observation points. For $y > y'$, trajectories corresponding to various indexes j are shown in Fig. 3. Field solutions pertaining to $j = 2,3,4$ take a form similar to those for $j = 1$. The index s counts the number of reflections experienced by the ray during its travel from $\boldsymbol{R}'$ to $\boldsymbol{R}$. Note that the trajectory defined by (22) includes a lateral shift at the boundaries. For each index sj in (21), the form of the result depends on whether the ray is reflected at the boundaries or is turned back by refraction before reaching the boundaries. The expressions in (21a)–(21c) pertain to the former case. When the ray is refracted and does not reach the boundary at y_1, there is no lateral shift but contact with a caustic (Fig. 4). In this case, one employs the phase change $\phi_1 = -\pi/2$ in (21b); in (21c), one puts $\partial^2\phi_1/\partial\tau_s^2 = 0$, and understands the imaginary part of the square root to be chosen as nega-

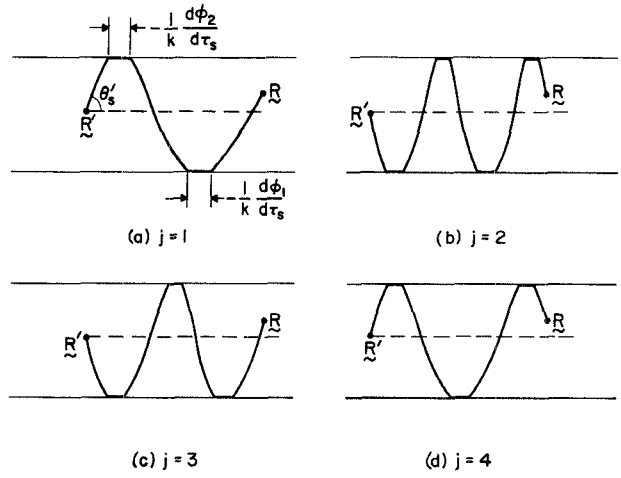

Fig. 3. Trajectories of rays that strike both boundaries. The trajectories are defined by ray equations, e.g., (22) for $j = 1$, and include a lateral shift $(-1/k)d\phi_1/d\tau_s$ or $(-1/k)d\phi_2/d\tau_s$ at each reflection. When the source point has the complex value in (10), the trajectory with $\theta_s' = \alpha$ defines the beam axis.

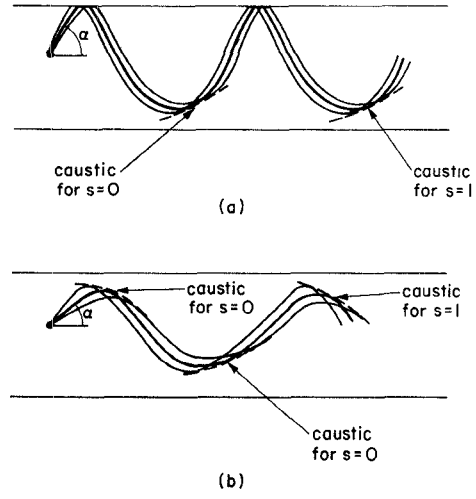

Fig. 4. Trajectories of rays that do not strike both boundaries. The trajectories are defined by ray equations modified as stated in the text. There is no lateral shift due to contact with a caustic. When the source point has the complex value in (10), the dark trajectories define the beam axis. (Two figures are omitted here, which describe rays leaving the source in the direction $y < y'$). (a) Contact with one boundary. (b) Contact with neither boundary.

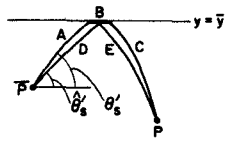

Fig. 5. Ray paths with and without lateral shift.

tive when the quantity inside the braces is negative (i.e., for rays beyond the turning-point but before touching the caustic; after a ray has touched the caustic, the quantity inside the braces is positive). Moreover, y_1 in (21a) is replaced by y_s where y_s, the y-coordinate of the turning-point at which the ray is horizontal, is defined by $n(y_s) = \tau_s$ (care must now be exercised in the calculation of $\partial^2\psi_{s1}/\partial\tau^2$; see [8]). Analogous considerations apply when the ray is refracted before striking the boundary at y_2. The angle θ_s of the ray trajectory with the positive z-axis is inferred from Snell's law

$$n(y) \cos [\theta_s(y)] = \tau_s = \text{constant}. \tag{23}$$

Thus the angle of departure θ_s' of the ray at the source is obtained from $n(y') \cos \theta_s' = \tau_s$. It should be noted that the classical ray tracing procedure can be adapted to the shifted ray paths, and that the field in (21), etc., away from the caustics (i.e., when S_{s1} is finite) can be constructed entirely by ray methods that utilize the phase contribution along the shifted paths and energy conservation in the corresponding tubes of rays [6], [7]. The ray tube cross section varies inversely with S_{s1}^2.

When the second exponential in (20a) is regarded as an amplitude factor, the stationary phase result for I_{s1} is again given by (21), with the following modifications: 1) ϕ_1 and ϕ_2 in (21c) are replaced by zero; and 2) the ray equation (stationary phase condition) in (22) is replaced by

$$\frac{\partial}{\partial \hat{\tau}_s} \psi_{s1}(\hat{\tau}_s) = 0 \tag{24}$$

and τ_s everywhere is replaced by $\hat{\tau}_s$. Thus (24) defines the classical ray path without lateral shift, and (21) then yields the conventional ray-optical field. Evidently, $\tau_s \neq \hat{\tau}_s$ for trajectories passing through $\boldsymbol{R}'$ and $\boldsymbol{R}$. It is of interest to examine how the fields calculated from (21) along a laterally shifted path (ABC in Fig. 5) differ from those along the classical path (DE in Fig. 5). For a single reflection, it is shown in Appendix I that when

$$\left(\frac{d\phi}{d\hat{\tau}_s}\right)^2 \left\{2k \left(\int_{y'}^{\bar{y}} + \int_{y}^{\bar{y}}\right) \frac{n^2(\xi)\, d\xi}{[n^2(\xi) - \hat{\tau}_s^2]^{3/2}}\right\}^{-1} \ll 1 \tag{25}$$

where $\bar{y}$ is the coordinate at the boundary, both methods of calculation yield the same result. For the special case of a homogeneous medium with n = constant, (25) reduces to

$$\frac{n \sin^2 \hat{\theta} (d\phi/d\hat{\tau}_s)^2}{2kQ} \ll 1 \qquad \hat{\tau}_s = n \cos \hat{\theta} \tag{25a}$$

where Q is the total path length along the incident and reflected rays, and $\hat{\theta}$ is the angle of departure of the classical ray path at the source. Thus, for large kQ and bounded $(d\phi/d\hat{\tau})$, one may compute the singly-reflected field by either method. The agreement continues to hold for a moderate number of multiple reflections where $d\phi/d\hat{\tau}_s$ in the inequality of (25) or (25a) is multiplied by s and the quantity inside the braces or Q is modified to account for multiply reflected paths. However, discrepancies will arise for large values of s when the above inequalities are no longer satisfied. Since the field in the waveguide is synthesized by ray contributions that have experienced many reflections, it may be anticipated that use of the shifted path is required; when s is large, the second exponential in the integrand of (20a) gives rise to rapid phase variations that must be included in the stationary phase calculation. This expectation is confirmed when the multiply-reflected ray contributions are converted into guided modes.

The conversion is accomplished by the Poisson transformation, which expresses a sum of functions in terms of a sum of their Fourier transforms. Since the sum over s in (20) starts from $s = 0$, the relevant form of the Poisson sum formula is

$$\sum_{s=0}^{\infty} F(2\pi s) = \frac{1}{2\pi} \sum_{m=-\infty}^{\infty} \int_{0^-}^{\infty} F(\zeta) \exp(-im\zeta)\, d\zeta. \tag{26}$$

The required analytic dependence on the summation index s is evidently satisfied by the functions I_{sj} in (21). When (26) is applied to (20), with (21), and also to the contributions from the other ray types j = 2,3,4, the resulting integrals can be evaluated by the stationary phase method. The procedure has been described previously [5]. It is found that, for large observation distances z, the Poisson-transformed ray series yields the asymptotic approximation of the exact guided mode series (18). The asymptotic approximation here implies that the eigenfunctions $\Phi_m(y)$ are replaced by their Wentzel–Kramer–Brillouin (WKB) forms, which describe the mode behavior in a slowly varying medium:

$$\Phi_m(y) \sim A_m^*(y) + i \exp\left\{i\phi_1 - 2ik \int_{y_{1m}}^{y_1} [n^2(\xi) - \tau_m^2]^{1/2}\, d\xi\right\} A_m(y) \tag{27}$$

where y_{1m} is defined by $n(y_{1m}) = \tau_m$,

$$A_m(y) = [n^2(y) - \tau_m^2]^{-1/4} \cdot \exp\left\{ik \int_{y_{1m}}^{y} [n^2(\xi) - \tau_m^2]^{1/2}\, d\xi - i\pi/4\right\} \tag{27a}$$

and the asterisk denotes the complex conjugate. These formulas are valid when the modal turning point y_{1m} is not contained in the layer region $y_1 < y < y_2$ (i.e., the mode field fills the entire cross section (Fig. 6(a)). When the mode field is refracted before reaching the boundary at y_1 (Fig. 6(b)), one has

$$\Phi_m(y) \sim A_m^*(y) + A_m(y) \qquad y_{1m} < y < y_2 \tag{28}$$

and when the mode field is trapped entirely by refraction (Fig. 6(c)), (28) applies as well in the region $y_{1m} < y < y_{2m}$. In regions $y_1 < y < y_{1m}$ of Fig. 6(b) and $y_1 < y < y_{1m}$, $y_{2m} < y < y_2$ of Fig. 6(c), the mode fields are evanescent and will not be treated further (for their evaluation, see [5]). The eigenvalues τ_m for modes characterized by Fig. 6(a) satisfy the resonance equation (modal dispersion relation) as specified by the saddle point condition in the integral (26) when applied to (20), with (21) (see [5, eqs. (I.30) and (I.15a)]):

$$[\phi_1(\tau_m) + \phi_2(\tau_m)] + 2k\int_{y_1}^{y_2} [n^2(\xi) - \tau_m^2]^{1/2}\, d\xi = 2\pi m \tag{29}$$

where m is a positive integer. For modes described by Fig. 6(b), one replaces ϕ_1 in (29) by the mode caustic phase shift $(-\pi/2)$ and y_1 by y_{1m}. For modes described by Fig. 6(c), one replaces ϕ_1 and ϕ_2 by $(-\pi/2)$, y_1 by y_{1m}, and y_2 by y_{2m}. When ϕ_1 or ϕ_2 are replaced by $(-\pi/2)$, it is implied that the caustic lies far enough from the waveguide boundaries to render evanescent field interaction with these boundaries negligible; if this is not the case, one must retain a corrected form of $\phi_{1,2}$. Finally, the normalization factor is found to be (see [5, eq. (I.19)]):

$$-2ik\tau_m N_m^2 \sim -4ikR_{1m}D_m(y_1,y_2;\phi_1,\phi_2), \quad \text{for Fig. 6(a)} \tag{30a}$$

$$\sim -4ikD_m(y_{1m},y_2;-\pi/2,\phi_2), \quad \text{for Fig. 6(b)} \tag{30b}$$

$$\sim -4ikD_m(y_{1m},y_{2m};-\pi/2,-\pi/2), \quad \text{for Fig. 6(c)} \tag{30c}$$

where R_{1m} is the factor multiplying $A_m(y)$ in (27), and

$$D_m(a,b;\phi_1,\phi_2) = \int_a^b \frac{\tau_m\, d\xi}{[n^2(\xi) - \tau_m^2]^{1/2}} - \frac{1}{2k}\frac{\partial}{\partial \tau_m}(\phi_1 + \phi_2). \tag{30d}$$

The asymptotically approximated mode series then follows from (18) on substitution of the three types of mode fields corresponding to Fig. 6(a)–(c); when the refractive index profile is such as to eliminate mode trapping as in Fig. 6(b) and (or) (c), one omits the corresponding modal contribution.

The modal resonance equation (29), or any of its modified forms as discussed above, represents the asymptotic approximation (in a slowly varying medium) of the rigorous equation for the modal eigenvalues (see [5, eq. (I.12)]). This result was obtained by converting the field contributions described by laterally shifted ray trajectories into modal form. With reference to the asymptotic evaluation of integral expressions for the field, it has been necessary to include the $\exp[iP_{sj}(\phi_1,\phi_2)]$ term in the phase of the integrands when dealing with (20a) and (26). If this term is not included in the phases of (20a) and (26) (corresponding to use of the classical geometric-optical ray paths in (24)), then one may show that the resulting resonance equation is

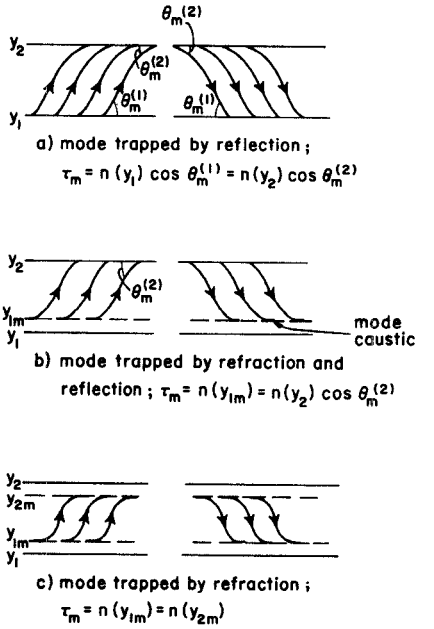

Fig. 6. Upgoing and downgoing ray congruences for trapped modes. (a) Mode trapped by reflection. (b) Mode trapped by refraction and reflection. (c) Mode trapped by refraction. The boundary y_1 in (b) and the boundaries y_1 and y_2 in (c) may be removed without substantially affecting the mode behavior.

$$k\int_{y_1}^{y_2} [n^2(\xi) - \hat{\tau}_m^2]^{1/2}\, d\xi = m\pi \tag{31}$$

which differs from the correct form in (29) whenever $\phi_{1,2} \neq 0$. If the $\exp[iP_{sj}(\phi_1,\phi_2)]$ term is excluded from the phase of (20a) but included in the phase of (26), one obtains a resonance equation as in (29), but with an additional term that causes the equation to be dependent on the source and observation point coordinates. While this additional term may be negligible under certain conditions, the formulation suffers from internal inconsistencies.

It has thus been shown that conversion of source-excited ray fields into modal fields requires use of laterally shifted ray trajectories. Since the ray trajectories emanating from the source also describe the local energy flow, and since the shifted trajectories are required for extraction of the correct modal dispersion equation, it may be expected that the group velocity of a modal field is consistent with tracking along shifted modal rays that are defined by the characteristic angle $\theta_m = \cos^{-1}[n(y)/\tau_m]$. This has been confirmed recently by an alternative analysis of modal fields in a homogeneous layer [9].

B. Beam Fields in an Inhomogeneous Layer with Impedance Walls

When the real source point $\boldsymbol{R}' = (y',z')$ is replaced by the complex source point $\boldsymbol{R}_b' = (y_b',z_b')$ in (10), the incident field in a weakly inhomogeneous medium may be inferred from the $s = 0$ term in (21), with $y_<$ and $y_>$ replaced by y_b' for $y > y_o$ and $y < y_o$, respectively. The

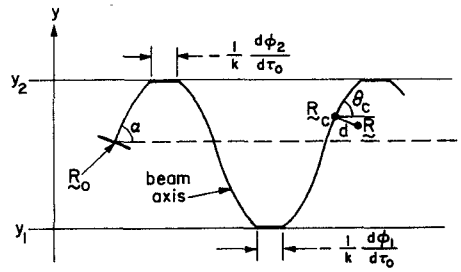

Fig. 7. Coordinates for calculation of paraxial beam field: $y = y_c - d\cos\theta_c$, $z = z_c + d\sin\theta_c$.

parameter τ_s defined in (22) is now complex; we shall denote $\tau_s \equiv \tau_b$ when $b \neq 0$. If the medium near $\boldsymbol{R}_o$ varies negligibly over a length interval equal to $b\sin\alpha$, one may approximate $n(y') \approx n(y_o)$ and

$$\int_{y_0+ib\sin\alpha}^{y} [n^2(\xi) - \tau_s^2]^{1/2}\, d\xi \approx \int_{y_0}^{y} [n^2(\xi) - \tau_s^2]^{1/2}\, d\xi - ib[n^2(y_o) - \tau_s^2]^{1/2}\sin\alpha. \tag{32}$$

It may then be verified by direct substitution that $\tau_b = \tau_o = n(y_o)\cos\alpha$ is a (real) solution of (22) when the observation point $\boldsymbol{R} = \boldsymbol{R}_c$ lies on the ray that leaves the point $\boldsymbol{R}_o$ along the $\boldsymbol{b}$ direction. This ray is the beam axis (see Figs. 3, 4, and 7) on which $|\exp(ik\psi_{s1})|$ assumes its maximum value. For complex τ_b corresponding to observation points off the beam axis, $|\exp(ik\psi_{s1})|$ decreases, and in the paraxial region near the beam axis, the decay is Gaussian. This property is maintained when $s \neq 0$ so that the representation in (21) yields a multiply reflected beam solution in an inhomogeneous layer. For observation points near the beam axis, the solution for I_{s1} in (21) is simplified to (see Appendix II):

$$I_{s1}(\tau_b) \sim S_{s1}(\tau_b)\exp[ik\psi_{s1}(\tau_b)] \cdot \exp\{is[\phi_1(\tau_o) + \phi_2(\tau_o)]\} \tag{33}$$

where

$$\psi_{s1}(\tau_b) = \psi_{s1}(\boldsymbol{R}_c,\boldsymbol{R}_o,\tau_o) - ibn(y_o) + \frac{d^2}{2\sin^2\theta_c}\left[E - \frac{ib}{n(y_o)\sin^2\alpha}\right]^{-1} \tag{33a}$$

$$S_{s1}(\tau_b) \approx \frac{\exp(i\pi/4)}{(8\pi k)^{1/2}}\left\{-n(y_c)n(y_o) \cdot \sin\theta_c\sin\alpha\left[-E + \frac{ib}{n(y_o)\sin^2\alpha}\right]\right\}^{-1/2} \tag{33b}$$

$$E = -\frac{\partial^2}{\partial\tau_o^2}\psi_{s1}(\boldsymbol{R}_c,\boldsymbol{R}_o,\tau_o) - \frac{s}{k}\frac{\partial^2}{\partial\tau_o^2}(\phi_1 + \phi_2). \tag{33c}$$

If the phase function in (21a) is denoted by $\psi_{s1}(\boldsymbol{R},\boldsymbol{R}',\tau_s)$, one may infer therefrom the phase function $\psi_{s1}(\boldsymbol{R}_c,\boldsymbol{R}_o,\tau_o)$ in (33a) and (33c). The various geometrical parameters are defined in Fig. 7, with d representing a distance measured perpendicularly from the beam axis. The exponential amplitude of the field is obtained from (33a) as

$$|\exp(ik\psi_{s1})| = \exp[kbn(y_o) - d^2/W^2] \tag{34}$$

where the squared $1/e$ beam width W^2 is given by

$$W^2 = \frac{2}{kb}n(y_o)\left[E^2 + \frac{b^2}{n^2(y_o)\sin^4\alpha}\right]\sin^2\alpha\sin^2\theta_c. \tag{34a}$$

The results above apply to the case where the beam is reflected at both boundaries. From (34a), the beam width expands with E, which quantity is proportional to $(1/\sin\theta_c)$ times the cross section of the tube of rays surrounding the beam axis when the excitation is due to a line current source (see comment after (23)). The remaining quantities in (33) are likewise those encountered in the ray optical treatment of the line source field. Thus the phase and amplitude behavior of the paraxial beam field may be inferred completely from the parameters describing the line-source-excited ray-optical field along the ray that coincides with the beam axis. Evidently, the directive properties of the beam source discriminate against some of the ray species in Fig. 3 in a manner analogous to that discussed in connection with Fig. 2. The utility of the multiply-reflected beam solution may also be assessed in the same fashion as described in connection with (14).

When the beam axis is refracted before reaching one or both boundaries (Fig. 4), the field is still given by (33) provided that one makes the modifications noted after (22). The manner of derivation of the paraxial formulas in Appendix II invalidates the solution when the beam axis becomes horizontal; however, (33) can be applied to observation regions corresponding to nonhorizontal beam directions. Since the line-source-excited ray system possesses caustics whereon the ray tube cross section vanishes [$E \to 0$ and hence $S_{s1}(\tau_s) \to \infty$ in (21c)], the ray-optical solution (21) cannot be employed there (due to the coalescence of two stationary points when the observation point approaches a caustic, one requires a uniform evaluation of the integral in (20a); see [13]). However, the complex-source-point solution in (33) remains bounded when $E \to 0$ and therefore still furnishes the beam field behavior. From (34a) vanishing values of E imply minimum (z-projected) beam widths so that the beam focuses whenever the beam axis touches a caustic (or a focus). Thus the line-source-excited ray system and its caustics or foci provide direct and quantitative information on the periodic expansion and focusing properties of beams that are trapped by the refractive index inhomogeneity in the layer. Because of the periodic focusing, the field representation in (33) is adequate for long propagation distances and thus preferable to the guided mode expansion.

The excitation of guided modes by the incident beam is obtained on replacing y' and z' in (18) by y_b' and z_b', respectively, in (10). In view of the assumption of slow variation of $n(y)$ over a length interval equal to the projected beam parameter $b \sin \alpha$, one may replace $\Phi_m(y')$ by its asymptotic forms in (27), (28), etc., and reduce the integrals as in (32). It is then found that the field solution for $z > z_o + b \sin \alpha$ is given by (see also [5, eqs. (I.34) and (I.39)]):

$$\bar{G}(\boldsymbol{R},\boldsymbol{R}_b') = \sum_m \frac{B_m}{-2ik\tau_m N_m^2} \Phi_m(y) \exp [ik\tau_m(z - z_o)] \tag{35}$$

where

$$B_m = f(\theta_m')u_1(y_o,\tau_m) + f(-\theta_m')u_2(y_o,\tau_m) \tag{35a}$$

$$u_{1,2}(y_o,\tau_m) = \frac{1}{2}\left[\Phi_m(y_o) \mp \frac{d\Phi_m(y_o)/dy_o}{ikn(y_o) \sin \theta_m'}\right] \tag{35b}$$

and

$$f(\theta_m') = \exp [kbn(y_o) \cos (\alpha - \theta_m')]$$

$$\cos \theta_m' = \tau_m/n(y_o). \tag{35c}$$

Note that u_1 and u_2 are traveling wave functions propagating along the $(-y)$ and $(+y)$ directions, respectively. As in (15), the beam acts like a directive source with radiation pattern $f(\theta)$ in a medium whose uniform properties are the same as the local properties of the inhomogeneous layer near the focus at $\boldsymbol{R}_o$. The most strongly excited modes are those whose propagation angles at $\boldsymbol{R}_o$ are closest to the beam angle α. If $\alpha \not\approx 0$, one may make further simplifications as in (13). It should be emphasized that while (35) is based on the assumption of a medium with negligible variation over the equivalent source region near $\boldsymbol{R}_o$, the medium variation elsewhere may be arbitrary. When the medium varies slowly everywhere, Φ_m and N_m^2 may be replaced by their asymptotic approximation in (27), etc., and (30).

C. Beam Fields in an Inhomogeneous Layer with Transparent Walls

When the layer is separated from a surrounding low refractive index medium by interfaces at $y_{1,2}$ across which the refractive index is discontinuous, the spectrum of modes guided along z contains a discrete and a continuous part. Some of the rays in Figs. 3 and 4(a) that reach the boundaries will now give rise to transmitted as well as reflected rays. However, rays that strike the boundaries at incidence angles larger than the critical angle are totally reflected, and their behavior is the same as for reflection at an impedance boundary provided that ϕ_1 and ϕ_2 denote the phases of the reflection coefficients for the transparent interface. When the incident field is a totally reflected beam, the fields corresponding to the lateral wave and the fields that penetrate the exterior region are weakly excited and hence negligible (see Appendix III and Fig. 8). The lateral wave fields are excited by the ray that impinges at the critical angle of total reflection, and they shed energy back into the slab region. Even when the source is an isotropic line source, these fields, contributed by the continuous mode spectrum, are $O(kz)^{-3/2}$ with respect to the guided modes and are therefore negligible at large distances. The highly directive beam source further weakens their contribution when the (totally reflected) beam axis is not near the critical direction. Therefore, the fields in the layer are still given by (33) or by the modal expansion in (35); concerning the latter, the Φ_m are now the eigenfunction for the inhomogeneous slab region.

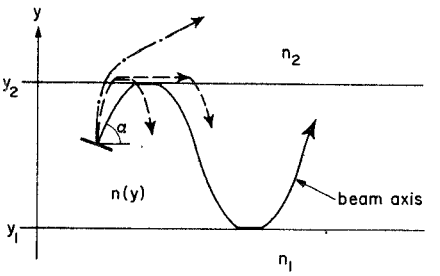

Fig. 8. Inhomogeneous layer with transparent walls. The refractive indexes for the exterior media satisfy the conditions $n_1 < n(y_1)$, $n_2 < n(y_2)$. The lateral rays (dashed) and external refracted rays (dot-dashed) are weakly excited when the beam axis strikes the interfaces at angles greater than the critical angle for total reflection.

V. SUMMARY

We have presented a study of the fields in a bounded inhomogeneous layer when the incident field is a Gaussian beam. The problem has been analyzed by a new method, the complex-source-point technique, which converts exact cylindrical wave solutions or asymptotic ray solutions into exact or asymptotic two-dimensional beam solutions. For this reason, detailed consideration has been given to the Green's function problem and to alternative representations of the line-source-excited fields. After it has been established that a particular Green's function representation can be continued analytically into a range of complex source coordinates, the resulting solution provides the beam-excited field without further calculation. The present investigation has been restricted to configurations wherein the medium properties vary negligibly over the equivalent source region representative of the complex location; in this case, the incident beam is Gaussian and the beam axis follows a geometric-optical ray trajectory. The nature of the fields excited by a source at a complex location when the medium varies appreciably over the equivalent source region remains to be further explored.

Two different formulations have been employed that represent the field either in terms of multiple reflections between the layer boundaries or in terms of guided modes. The utility of each, and the conversion from one to the other, has been analyzed, and it has been shown how the

cumulative effect of ray fields with many reflections can be expressed in modal form. Because a well-collimated beam represents a highly directive source, the complex-source-point results have been related also to a previous study that dealt with the radiation from a directive source distribution into a layered medium [5]. While both methods yield the same expression for the excitation of modal fields, it has been noted that the complex-source-point method is more versatile in being able to deal also with other aspects of the beam problem.

Since the present analysis treats the complete excitation problem by a localized source, it is sufficiently general to clarify the interrelation and interpretation of various ray and beam propagation processes that have usually been considered individually under less general conditions. The following conclusions are worthy of emphasis.

1) When a boundary has an incidence-angle-dependent reflection coefficient, the amplitude and phase of the line-source-excited reflected field may be computed either by the conventional geometric-optical method based on the classical incident and reflected ray trajectories, or by a modified geometric-optical method that utilizes a laterally shifted path. The laterally shifted and conventional ray paths correspond to the inclusion, or not, of the reflection coefficient phases into the phase of the wave bundle that synthesizes the ray field. When the field experiences many reflections, the reflection coefficient phases must be so included whence the laterally shifted path is generally required.

2) When the multiply reflected ray fields in a plane stratified layer are converted to modal form, the correct modal dispersion equation is obtained from the laterally shifted ray path model. Omission of the lateral shift generally leads to an incorrect dispersion equation.

3) Beam optics and source-excited ray optics have been shown to be accommodated by the same formulation, distinguished only by whether or not the source point location is complex. The beam axis coincides with a real ray trajectory. The paraxial beam field has a Gaussian variation, but the solution remains valid also outside the paraxial region. In this respect, the complex-source-point method differs from other methods (for example, [11]) wherein the paraxial regime and Gaussian behavior are *assumed* at the outset. The field properties in the paraxial region can be inferred completely from those of the paraxial tube of real rays, which is generated by a line source located at the beam focus (see (33)). In particular, the beam cross section expands and contracts with the paraxial ray tube surrounding the beam axis. Thus the method provides a particularly simple and quantitative connection between paraxial beams and source-excited paraxial rays.

4) When the line-source-excited ray field is trapped by refraction instead of reflection, the ray family exhibits caustics or foci. Maximum contraction of the z-projected beam cross section takes place when the axis touches a caustic or focus of the paraxial ray system. While the asymptotic ray field solution due to a line source at a real location fails at a caustic or focus, the complex-source-point (beam) solution remains valid at these real observation points.

5) The complex-source-point method converts line-source-excited fields into beam fields even when an initially paraxial beam is strongly scattered by localized scattering centers or by strong medium inhomogeneity. Examples of the former process have been given elsewhere [4], [10]; applicability of the latter is illustrated by the modal excitation result in (35).

Extension of the method to three-dimensional configurations is straightforward. One must now examine three-dimensional scalar and dyadic Green's functions for scalar and vector fields, respectively, and assign to the source point a complex location as discussed in Section II. While applications to three dimensions are still under study, it is to be expected that the general behavior of alternative representations of the beam fields deduced in this manner will be analogous to that discussed here for the two-dimensional case.

APPENDIX I
FIELD EVALUATION ALONG CONVENTIONAL REFLECTED AND LATERALLY SHIFTED PATHS

Referring to Fig. 5, with $\bar{P} = (y',z')$ and $P = (y,z)$, the phase along the conventional path DE is given by

$$\psi(\hat{\tau}_s) = \left(\int_{y'}^{\bar{y}} + \int_{y}^{\bar{y}}\right)[n^2(\xi) - \hat{\tau}_s^2]^{1/2}\, d\xi + \hat{\tau}_s(z - z') \quad (36)$$

with $\hat{\tau}_s$ defined by $\partial\psi/\partial\hat{\tau}_s = 0$. The phase along the laterally shifted path ABC is

$$\bar{\psi}(\tau_s) = \psi(\tau_s) + (1/k)\phi(\tau_s) \quad (37)$$

where ϕ is the phase of the boundary reflection coefficient and τ_s is defined by $\partial\bar{\psi}/\partial\tau_s = 0$. Since $\tau_s \approx \hat{\tau}_s$ (we shall assume that $d\phi/d\tau_s$ and $d^2\phi/d\tau_s^2$ do not become excessively large), one obtains by perturbation expansion that

$$\hat{\tau}_s - \tau_s \approx \frac{d\phi/k\; d\hat{\tau}_s}{\partial^2\bar{\psi}/\partial\hat{\tau}_s^2} \approx \frac{d\phi/k\; d\hat{\tau}_s}{\partial^2\psi/\partial\hat{\tau}_s^2}. \quad (38)$$

When the expression for $\tau_s = \hat{\tau}_s + \delta$ is substituted into (37) and the phase is expanded to $O(\delta^2)$, one finds that $\psi(\hat{\tau}_s) = \bar{\psi}(\tau_s)$, subject to the restriction in (25) and those noted above.

An interesting observation follows when the complex source point is used to convert the line source field into an incident beam field. It has been found previously [12] that use of the resulting complex value of $\hat{\tau}_s$ in the field expression derived from the *nonshifted* path predicts correctly the lateral Goos-Hänchen beam shift for a single reflection. It then follows that a modification of this result might occur when one calculates the reflected beam field from the complex value of τ_s corresponding to the laterally shifted path. However, because of the equivalence shown above, the discrepancy is found to be neg-

ligible for a single or a small number of reflections. For a large number of reflections, the laterally shifted path is required.

APPENDIX II
SOLUTION FOR τ_s IN PARAXIAL REGION

Let $\bar{\psi}(\boldsymbol{R},\boldsymbol{R}_b',\tau)$ denote the total phase so that (22) is written $\partial\bar{\psi}/\partial\tau_s = 0$. Referring to Fig. 7, we expand $\bar{\psi}$ near the beam center as

$$\bar{\psi}(\boldsymbol{R},\boldsymbol{R}_b',\tau) = \bar{\psi}(\boldsymbol{R}_c,\boldsymbol{R}_b',\tau_o) + \frac{\partial\bar{\psi}}{\partial d}d + \frac{\partial\bar{\psi}}{\partial\tau_o}(\tau-\tau_o) + \frac{\partial^2\bar{\psi}}{\partial\tau_o\,\partial d}d(\tau-\tau_o) + \frac{1}{2}\frac{\partial^2\bar{\psi}}{\partial\tau_o^2}(\tau-\tau_o)^2 + \cdots \tag{39}$$

where all derivatives are evaluated at $\tau = \tau_o$, $\boldsymbol{R} = \boldsymbol{R}_c$, $d = 0$. Note that $(\partial\bar{\psi}/\partial\tau_o) = 0$ and $\partial\bar{\psi}/\partial d = 0$. Then from $\partial\bar{\psi}/\partial\tau_s = 0$, one finds

$$\tau_s - \tau_o = -d\,\frac{\partial^2\bar{\psi}/\partial\tau_o\,\partial d}{\partial^2\bar{\psi}/\partial\tau_o^2} \tag{40}$$

and, consequently,

$$\bar{\psi}(\boldsymbol{R},\boldsymbol{R}_b',\tau_s) = \bar{\psi}(\boldsymbol{R}_c,\boldsymbol{R}_b',\tau_o) - \frac{d^2}{2}\frac{(\partial^2\bar{\psi}/\partial\tau_o\,\partial d)^2}{\partial^2\bar{\psi}/\partial\tau_o^2} + \cdots. \tag{41}$$

When the various derivatives of $\bar{\psi}$ are evaluated, one obtains the result in (33). The validity of the expansion (39) requires that all $\bar{\psi}$ derivatives are bounded. Since $\partial^2\bar{\psi}/\partial\tau_o\,\partial d = \csc\theta_c$, this restricts applicability of the result to beam axis directions that deviate from the horizontal (unless $d \to 0$).

APPENDIX III
VALIDITY OF COMPLEX-SOURCE-POINT METHOD FOR LAYER WITH TRANSPARENT BOUNDARIES

When the line source is located inside the layer, the eigenfunction expansion (plane wave spectral decomposition) with respect to z in [5, eq. (I.8)] remains applicable. However, in addition to spectral pole singularities of the resonance denominator (spectral poles exist only when the layer can support trapped, nonleaky modes), the integrand also contains branch point singularities. When the integration path in the complex τ-plane is deformed around these singularities, one obtains a representation in terms of eigenfunctions in y, which now includes a discrete spectrum of modes as in [5, eq. (I.13a)], corresponding to the pole singularities, and a continuous spectrum of modes arising from the branch points. The theory describing these field representations may be found in the literature [8, secs. 5.6 and 5.8], [13] (references in this Appendix refer to a homogeneous layer; inhomogeneity does not alter the basic conclusions).

It can be shown that these field representations as well as the multiple reflection representation in [5, eq. (I.21)] based on the expansion in [5, eq. (I.20)], remain convergent and hence valid when (y',z') is replaced by (y_b',z_b') in (10). For representations involving eigenfunctions in z, one must impose the restriction $y > y_o + b\cos\alpha$ (for the multiple reflection representation, only the incident field term must be so restricted); for representations involving eigenfunctions in y, one requires $z > z_o + b\sin\alpha$. These are the previously stated conditions that describe the equivalent source region in the y and z domains, respectively. It can also be shown that the asymptotic results obtained for various integrals are the same as when (y_b',z_b') is substituted for (y',z') in the asymptotic solutions for the line source field. This observation applies in particular to the continuous spectrum contribution to the field expressed in terms of modes propagating along z. It is known [13] that this contribution, descriptive of lateral waves (see Fig. 8), is $O[k(z-z')]^{-3/2}$ with respect to the guided waves excited by a line source. This justifies omission of the continuous spectrum contribution as noted in Section IV-C.

When the line source is located outside the layer, the preceding considerations are applied to the Green's function representations modified so as to account for the changed source position [8, secs. 5.6 and 5.8].

REFERENCES

[1] S. E. Miller, E. A. J. Marcatili, and T. Li, "Research toward optical fiber transmission systems," *Proc. IEEE*, vol. 61, pp. 1703–1751, Dec. 1973.

[2] D. Marcuse, *Light Transmission Optics*. New York: Van Nostrand Reinhold, 1972.

[3] G. Deschamps, "The Gaussian beam as a bundle of complex rays," *Electron. Lett.*, vol. 7, pp. 684–685, 1971.

[4] L. B. Felsen, "Complex-source-point solutions of the field equations and their relation to the propagation and diffraction of Gaussian beams," to be published in *Symposia Matematica (Proc. Symp. Mathematical Theory of Electromagnetism*, Rome, Italy, Feb. 19–22, 1974).

[5] D. V. Batorsky and L. B. Felsen, "Ray-optical calculation of modes excited by sources and scatterers in a weakly inhomogeneous duct," *Radio Sci.*, vol. 6, pp. 911–923, 1971.

[6] D. V. Batorsky, "Radiation and scattering in weakly inhomogeneous ducts," Ph.D. dissertation, Dept. of Electrical Engineering and Electrophysics, Polytechnic Institute of Brooklyn, Brooklyn, N. Y., 1971.

[7] L. B. Felsen, "Asymptotic techniques for propagation and scattering in inhomogeneous waveguides and ducts," AGARD Conference Report No. CPP-144 on Electromagnetic Wave Propagation Involving Irregular Surfaces and Inhomogeneous Media, 1974, distributed by various National Distribution Centers of the Advisory Group for Aerospace Research and Development (AGARD).

[8] L. B. Felsen and N. Marcuvitz, *Radiation and Scattering of Waves*. Englewood Cliffs, N. J.: Prentice-Hall, 1973, p. 589.

[9] H. Kogelnik and H. P. Weber, "Rays, stored energy, and power flow in dielectric waveguides," *J. Opt. Soc. Amer.*, vol. 64, pp. 174–185, 1974.

[10] S. Choudhary and L. B. Felsen, "Analysis of Gaussian beam propagation and diffraction by inhomogeneous wave tracking," *Proc. IEEE (Special Issue on Rays and Beams)*, vol. 62, pp. 1530–1541, Nov. 1974.

[11] L. W. Casperson, "Gaussian light beams in inhomogeneous media," *Appl. Opt.*, vol. 12, pp. 2434–2441, 1973.

[12] J. W. Ra, H. L. Bertoni, and L. B. Felsen, "Reflection and transmission of beams at a dielectric interface," *SIAM J. Appl. Math.*, vol. 24, pp. 396–413, 1973.

[13] L. M. Brekhovskikh, *Waves in Layered Media*. New York: Academic, 1960, pp. 341–361.